Hyperbolic Feature Augmentation via Distribution Estimation and Infinite Sampling on Manifolds

Zhi Gao[1], **Yuwei Wu**[1,2]*, **Yunde Jia**[2,1], **Mehrtash Harandi**[3]
[1] Beijing Lab of Intellegent Information Technology, School of Computer Science,
Beijing Institute of Technology, China
[2] Guangdong Lab of Machine Perception and Intelligent Computing,
Shenzhen MSU-BIT University, China
[3] Department of Electrical and Computer Systems Eng.,
Monash University, and Data61, Australia
{gaozhi_2017,wuyuwei,jiayunde}@bit.edu.cn, mehrtash.harandi@monash.edu

Abstract

Learning in hyperbolic spaces has attracted growing attention recently, owing to their capabilities in capturing hierarchical structures of data. However, existing learning algorithms in the hyperbolic space tend to overfit when limited data is given. In this paper, we propose a hyperbolic feature augmentation method that generates diverse and discriminative features in the hyperbolic space to combat overfitting. We employ a wrapped hyperbolic normal distribution to model augmented features, and use a neural ordinary differential equation module that benefits from meta-learning to estimate the distribution. This is to reduce the bias of estimation caused by the scarcity of data. We also derive an upper bound of the augmentation loss, which enables us to train a hyperbolic model by using an infinite number of augmentations. Experiments on few-shot learning and continual learning tasks show that our method significantly improves the performance of hyperbolic algorithms in scarce data regimes.

1 Introduction

Several recent studies reveal that real-world data, such as images, videos, graphs, and sentences in natural language, usually endows a hierarchical structure [1]. In contrast to the Euclidean space with zero curvature, a hyperbolic space characterized by constant negative curvature can well capture such hierarchical structures, since the volume of the hyperbolic space grows exponentially with respect to the radius [2]. This property leads to rich representations and encourages successful developments of hyperbolic algorithms for various applications. Examples include image retrieval [3], action recognition [4], graph classification [5], and machine translation [6].

Although existing hyperbolic algorithms have achieved impressive performances, they often rely on the availability of sufficient data for training. In many practical applications, very limited data is given, as collecting and labeling data is costly. For example, in few-shot animal recognition [7, 8], animal images have hierarchical structures according to their species information. With few images (say less than five) in each class, training a model (*e.g.*, a ResNet combined with hyperbolic geometry [9, 3]) suffers from the undesirable overfitting problem. This motivates us to study combating overfitting with limited data in the hyperbolic space.

In this paper, we propose a hyperbolic feature augmentation (HFA) method that overcomes overfitting by generating class-identity-preserving features in the hyperbolic space. Compared with augmentation

*Corresponding author: Yuwei Wu

36th Conference on Neural Information Processing Systems (NeurIPS 2022).

in the original space of data (*e.g.*, image space), augmentation in the feature space requires less memory footprint [10, 11]. Moreover, feature augmentation is capable of providing useful intra-class variants by capturing diverse and discriminative augmentation directions, enabling the model to learn the invariance of each class [12, 13]. Therefore, feature augmentation offers a feasible way to overcome overfitting in the hyperbolic space.

Performing feature augmentation in the hyperbolic space involves two challenges. (1) The augmentation directions should be discriminative and reflect the variations of intra-class in the curved hyperbolic space rather than a flat space. The scarce data and complicated hierarchical structures make producing suitable augmentation directions non-trivial. (2) Augmentation in the hyperbolic space is computationally expensive (as compared to the Euclidean space), as the process of augmentation requires complex hyperbolic operations (*e.g.*, parallel transport and exponential map) to preserve the non-Euclidean geometry of augmented features.

We introduce a meta-neural-ODE distribution estimation scheme to solve the first challenge. We employ a wrapped normal distribution for augmented features, where the augmentation directions are sampled in the tangent bundle and projected to the hyperbolic space. We estimate the distribution by solving a continuous optimization process with neural ordinary differential equation (ODE), and utilize meta-learning to acquire prior knowledge in a gradient flow network for the estimation. The continuous optimization with prior knowledge leads to more reliable distribution for scarce data and complicated structures. We derive an upper bound of the augmentation loss to solve the second challenge, which enables us to train a hyperbolic model using an infinite number of sampled features. As a result, our method brings enhanced diversity of data and does not need to perform data augmentation explicitly, making an efficient augmentation algorithm without complex hyperbolic operations. We evaluate the proposed HFA method on few-shot learning and continual learning tasks, and results show that the proposed method significantly improves the performance of hyperbolic algorithms when limited data is given. The code of HFA is available at `https://github.com/ZhiGaomcislab/Hyperbolic_Feature_Augmentation`.

In summary, our contributions are threefold. **(1)** To the best of our knowledge, we are the first to perform feature augmentation in the hyperbolic space. The proposed HFA method is capable of generating diverse and discriminative hyperbolic features, addressing the overfitting problem. **(2)** We introduce a meta-neural-ODE distribution estimation scheme, whose continuous optimization process with prior knowledge leads to precise approximation of the real distribution in scarce data regimes. **(3)** We derive an upper bound of the augmentation loss to train a hyperbolic model using infinite augmentation, which creates an efficient augmentation algorithm without explicit augmentation and hyperbolic operations.

2 Related Work

Data augmentation. Data augmentation techniques, widely used to improve generalization, can be divided into two categories: **1.** augmentation in the original space of data (*e.g.*, image space) and **2.** augmentation in the feature space. Hand designed transformations (*e.g.*, masking and cropping) are popular examples from the first category [14, 15]. Automatic augmentation is a promising technique to automatically choose hand-crafted transformations [16, 17]. To produce more intra-class variants, some methods train a generative model for augmentation in the original space [18, 19]. One drawback of generating augmentation in the original space is the computational load of the algorithms. In contrast, feature augmentation not only brings rich intra-class variants but also involves less computational complexity and memory footprint. The benefits of feature augmentation are demonstrated for many applications, including but not limited to contrastive learning [20], domain adaptation [21], few-shot learning [22], long-tailed recognition [13], and instance segmentation [11]. Feature augmentation is usually achieved by manifold mixup [23, 24], sampling from captured distributions [25, 12, 10, 11], or utilizing a GAN model [26, 27]. Different from existing feature augmentation, we focus on augmentation in the hyperbolic space.In doing so, we introduce a meta-neural-ODE distribution estimation scheme, instead of directly computing distribution from given data. In this case, our method can better adapt to complex distributions in scarce data regimes.

Hyperbolic geometry. Learning in the hyperbolic space has become an alternative to the Euclidean space, since natural data usually exhibits hierarchical structures. Existing efforts of exploiting the hyperbolic space can be roughly divided into two categories: learning hyperbolic embeddings and designing hyperbolic neural networks. Methods of the first category add several hyperbolic operations on the top of a conventional neural network to obtain discriminative hyperbolic embeddings. This scheme has been used in many applications, such as image retrieval [3], few-shot learning [28], metric learning [29], and image segmentation [30]. The second category focuses on extending the entire architecture of a neural network to the hyperbolic space, such as hyperbolic convolutional network [6], hyperbolic graph network [31, 5], hyperbolic attention network [32], and hyperbolic variational autoencoder [33, 34]. These methods mainly focus on the model level of hyperbolic algorithms (*i.e.*, designing/improving hyperbolic models). In contrast, our method studies the data level of hyperbolic algorithms and efficiently improves the generalization of models via data augmentation.

3 Preliminaries

A hyperbolic space is a smooth Riemannian manifold with constant negative curvature [35]. Hyperbolic space has five isometric models, and we use the Poincaré ball model [36] to work with. A Poincaré ball is defined as $\mathcal{M}^{d,c} = \{\boldsymbol{x} \in \mathbb{R}^d, -c\|\boldsymbol{x}\| < 1\}$, where d is the dimension of vectors in the space, $\|\cdot\|$ is the Euclidean norm, and the curvature $c < 0$ represents the deviation of $\mathcal{M}^{d,c}$ from a flat space. For $\boldsymbol{u} \in \mathcal{M}^{d,c}$, its tangent space, denoted by $T_{\boldsymbol{u}}\mathcal{M}^{d,c}$, contains all tangent vectors to $\mathcal{M}^{d,c}$ at $\boldsymbol{u}$. We will make use of the following operations in our work;

Addition. For $\boldsymbol{x}, \boldsymbol{y} \in \mathcal{M}^{d,c}$, their addition is

$$\boldsymbol{x} \oplus_c \boldsymbol{y} = \frac{(1 - 2c\langle \boldsymbol{x}, \boldsymbol{y}\rangle_2 - c\|\boldsymbol{y}\|^2)\boldsymbol{x} + (1 + c\|\boldsymbol{x}\|^2)\boldsymbol{y}}{1 - 2c\langle \boldsymbol{x}, \boldsymbol{y}\rangle_2 + c^2\|\boldsymbol{x}\|^2\|\boldsymbol{y}\|^2}. \tag{1}$$

Distance measure. For two vectors $\boldsymbol{x}, \boldsymbol{y} \in \mathcal{M}^{d,c}$, their distance is

$$d^c(\boldsymbol{x}, \boldsymbol{y}) = \frac{1}{\sqrt{|c|}} \cosh^{-1}\left(1 - 2c\frac{\|\boldsymbol{x} - \boldsymbol{y}\|^2}{(1 + c\|\boldsymbol{x}\|^2)(1 + c\|\boldsymbol{y}\|^2)}\right). \tag{2}$$

Exponential map. The exponential map $\mathrm{expm}^c_{\boldsymbol{x}}(\boldsymbol{s})$ projects a vector $\boldsymbol{s}$ from the tangent space $T_{\boldsymbol{x}}\mathcal{M}^{d,c}$ to the manifold $\mathcal{M}^{d,c}$,

$$\mathrm{expm}^c_{\boldsymbol{x}}(\boldsymbol{s}) = \boldsymbol{x} \oplus_c \Big(\tanh(\sqrt{|c|}\frac{\lambda^c_{\boldsymbol{x}}\|\boldsymbol{s}\|}{2})\frac{\boldsymbol{s}}{\sqrt{|c|}\|\boldsymbol{s}\|}\Big), \tag{3}$$

where $\lambda^c_{\boldsymbol{x}} = 2/(1 + c\|\boldsymbol{x}\|^2)$ is the conformal factor. The exponential map in the tangent space $T_{\boldsymbol{0}}\mathcal{M}^{d,c}$ at the origin is simplified to $\mathrm{expm}^c_{\boldsymbol{0}}(\boldsymbol{s}) = \tanh(\sqrt{|c|}\|\boldsymbol{s}\|)\frac{\boldsymbol{s}}{\sqrt{|c|}\|\boldsymbol{s}\|}$.

Logarithmic map. The logarithmic map $\mathrm{logm}^c_{\boldsymbol{x}}(\boldsymbol{y})$ maps a vector $\boldsymbol{y}$ from the manifold to the tangent space $T_{\boldsymbol{x}}\mathcal{M}^{d,c}$,

$$\mathrm{logm}^c_{\boldsymbol{x}}(\boldsymbol{y}) = \frac{2}{\sqrt{|c|}\lambda^c_{\boldsymbol{x}}}\tanh^{-1}(\sqrt{|c|}\| - \boldsymbol{x} \oplus_c \boldsymbol{y}\|)\frac{-\boldsymbol{x} \oplus_c \boldsymbol{y}}{\| - \boldsymbol{x} \oplus_c \boldsymbol{y}\|}. \tag{4}$$

The exponential map $\mathrm{logm}^c_{\boldsymbol{0}}$ in $T_{\boldsymbol{0}}\mathcal{M}^{d,c}$ is simplified to $\mathrm{logm}^c_{\boldsymbol{0}}(\boldsymbol{y}) = \tanh^{-1}(\sqrt{|c|}\|\boldsymbol{y}\|)\frac{\boldsymbol{y}}{\sqrt{|c|}\|\boldsymbol{y}\|}$.

Parallel transport The parallel transport operation $\mathrm{PT}^c_{\boldsymbol{x}\to\boldsymbol{y}}(\boldsymbol{s}) : T_{\boldsymbol{x}}\mathcal{M}^{d,c} \to T_{\boldsymbol{y}}\mathcal{M}^{d,c}$ moves a vector from the tangent space $T_{\boldsymbol{x}}\mathcal{M}^{d,c}$ to another one $T_{\boldsymbol{y}}\mathcal{M}^{d,c}$ along the geodesic,

$$\mathrm{PT}^c_{\boldsymbol{x}\to\boldsymbol{y}}(\boldsymbol{s}) = \frac{\lambda^c_{\boldsymbol{x}}}{\lambda^c_{\boldsymbol{y}}}\mathrm{gyr}[\boldsymbol{y}, -\boldsymbol{x}]\boldsymbol{s}\ , \tag{5}$$

where $\mathrm{gyr}[\boldsymbol{y}, -\boldsymbol{x}]\boldsymbol{s} = -(\boldsymbol{x} \oplus_c \boldsymbol{y}) \oplus_c (\boldsymbol{x} \oplus_c (\boldsymbol{y} \oplus_c \boldsymbol{s}))$. This operation in $T_{\boldsymbol{0}}\mathcal{M}^{d,c}$ is $\mathrm{PT}^c_{\boldsymbol{0}\to\boldsymbol{y}}(\boldsymbol{s}) = \frac{2}{\lambda^c_{\boldsymbol{y}}}\boldsymbol{s}$.

4 Method

4.1 Formulation

In this paper, we propose the hyperbolic feature augmentation (HFA) method. We employ a wrapped normal distribution $\mathcal{P}(c, \boldsymbol{p}, \boldsymbol{\mu}, \boldsymbol{\Sigma})$ to model features in scarce data regimes, and meta-learn a neural

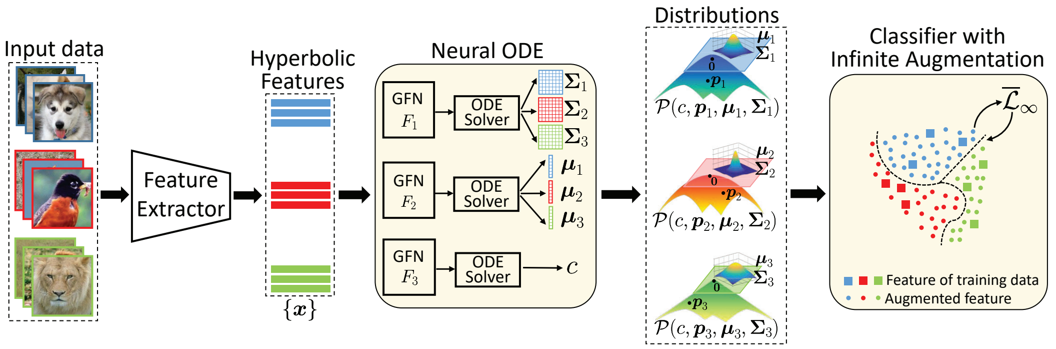
Input data
Feature Extractor
Hyperbolic Features
$\{\boldsymbol{x}\}$
Neural ODE
GFN F_1
GFN F_2
GFN F_3
ODE Solver
ODE Solver
ODE Solver
$\boldsymbol{\Sigma}_1$ $\boldsymbol{\Sigma}_2$ $\boldsymbol{\Sigma}_3$
$\boldsymbol{\mu}_1$ $\boldsymbol{\mu}_2$ $\boldsymbol{\mu}_3$
c
Distributions
$\mathcal{P}(c,\boldsymbol{p}_1,\boldsymbol{\mu}_1,\boldsymbol{\Sigma}_1)$
$\mathcal{P}(c,\boldsymbol{p}_2,\boldsymbol{\mu}_2,\boldsymbol{\Sigma}_2)$
$\mathcal{P}(c,\boldsymbol{p}_3,\boldsymbol{\mu}_3,\boldsymbol{\Sigma}_3)$
Classifier with Infinite Augmentation
$\overline{\mathcal{L}}_\infty$
Feature of training data
Augmented feature

Figure 1: A conceptual diagram of HFA. GFN denotes the proposed gradient flow network.

ODE to estimate a distribution for each class. Then, we derive an upper bound $\overline{\mathcal{L}}_\infty$ of the loss function with infinite augmentation to train the classifier. An illustration of main components of HFA is provided in Figure 1.

4.2 Wrapped Normal Distribution in Scarce Data Regime

The wrapped normal distribution has been successfully used in various studies to model distributions in Riemannian manifolds [37, 38, 39]. The underlying idea is to model a Riemannian distribution as a projection of a normal distribution on a tangent space to the manifold. Here, we introduce it to scarce data regimes. The density of a wrapped normal distribution is given by

$$\mathcal{P}(\boldsymbol{z}|c,\boldsymbol{p},\boldsymbol{\mu},\boldsymbol{\Sigma}) = \mathcal{N}(\lambda^c_{\boldsymbol{p}}\mathrm{logm}^c_{\boldsymbol{p}}(\boldsymbol{z})|\boldsymbol{\mu},\boldsymbol{\Sigma})\left(\frac{\sqrt{|c|}d^c(\boldsymbol{p},\boldsymbol{z})}{\sinh(\sqrt{|c|}d^c(\boldsymbol{p},\boldsymbol{z}))}\right), \tag{6}$$

where c is the curvature of the underlying space, $\boldsymbol{p} \in \mathcal{M}^{d,c}$ is the prototype of given data, and $\boldsymbol{\mu}$ and $\boldsymbol{\Sigma} \in \mathbb{R}^{d\times d}$ are the mean and the covariance matrix of augmentation directions, respectively. Since few data is given in scarce data regimes, the prototype $\boldsymbol{p}$ may be biased.

Generating a feature from $\mathcal{P}(c,\boldsymbol{p},\boldsymbol{\mu},\boldsymbol{\Sigma})$ includes three steps. (1) Sample a vector $\widehat{\boldsymbol{v}}$ from the normal distribution $\mathcal{N}(\boldsymbol{\mu},\boldsymbol{\Sigma})$ in the tangent space $T_{\boldsymbol{0}}\mathcal{M}^{c,d}$. (2) Transport $\widehat{\boldsymbol{v}}$ from $T_{\boldsymbol{0}}\mathcal{M}^{c,d}$ to $\boldsymbol{v}$ in the tangent space $T_{\boldsymbol{p}}\mathcal{M}^{c,d}$, $\boldsymbol{v} = \mathrm{PT}^c_{\boldsymbol{0}\to\boldsymbol{p}}(\widehat{\boldsymbol{v}})$. (3) Map $\boldsymbol{v}$ to the manifold by $\boldsymbol{z} = \mathrm{expm}^c_{\boldsymbol{p}}(\boldsymbol{v})$. In the step (1), sampling $\widehat{\boldsymbol{v}}$ from $\mathcal{N}(\boldsymbol{\mu},\boldsymbol{\Sigma})$ is not a differentiable process, and we can not back propagate gradients to $\boldsymbol{\mu}$ and $\boldsymbol{\Sigma}$. We use a reparameterization trick to solve this issue. We sample a vector $\boldsymbol{\epsilon}$ from the standard normal distribution $\mathcal{N}(\boldsymbol{0},\boldsymbol{I})$ and transform $\boldsymbol{\epsilon}$ to $\widehat{\boldsymbol{v}}$ by $\widehat{\boldsymbol{v}} = \boldsymbol{\mu} + \boldsymbol{L}\boldsymbol{\epsilon}$, where $\boldsymbol{L}\boldsymbol{L}^\top = \boldsymbol{\Sigma}$. The sampling process is summarized in Algorithm 1.

Algorithm 1 Sampling process in HFA.

```
Input: A wrapped normal distribution $\mathcal{P}(c,\boldsymbol{p},\boldsymbol{\mu},\boldsymbol{\Sigma})$,
    where $\boldsymbol{\Sigma}$ is decomposed by $\boldsymbol{L}\boldsymbol{L}^\top = \boldsymbol{\Sigma}$.
Output: $\boldsymbol{z} \in \mathcal{M}^{d,c}$ sampled from $\mathcal{P}$
1: Sample $\boldsymbol{\epsilon}$ from a standard normal distribution $\mathcal{N}(\boldsymbol{0},\boldsymbol{I})$.
2: Use the reparameterization trick to obtain $\widehat{\boldsymbol{v}} = \boldsymbol{\mu} + \boldsymbol{L}\boldsymbol{\epsilon}$.
3: Transport $\widehat{\boldsymbol{v}}$ from $T_{\boldsymbol{0}}\mathcal{M}^{c,d}$ to $T_{\boldsymbol{p}}\mathcal{M}^{c,d}$ by $\boldsymbol{v} = \mathrm{PT}^c_{\boldsymbol{0}\to\boldsymbol{p}}(\widehat{\boldsymbol{v}})$.
4: Map $\boldsymbol{v}$ to the manifold by $\boldsymbol{z} = \mathrm{expm}^c_{\boldsymbol{p}}(\boldsymbol{v})$.
```

We apply one wrapped normal distribution to each class. For the distribution $\mathcal{P}(c,\boldsymbol{p}_j,\boldsymbol{\mu}_j,\boldsymbol{\Sigma}_j)$ of the j-th class, its has its own prototype $\boldsymbol{p}_j$, mean $\boldsymbol{\mu}_j$, and covariance matrix $\boldsymbol{\Sigma}_j$. All classes share a common curvature c.

4.3 Distribution Estimation by Neural ODE

Neural ODE. For the wrap distribution $\mathcal{P}(c,\boldsymbol{p}_j,\boldsymbol{\mu}_j,\boldsymbol{\Sigma}_j)$, the prototype $\boldsymbol{p}_j$ can be computed by averaging given samples (*e.g.*, the Einstein midpoint [40]). We use a neural ODE to estimate c, $\boldsymbol{\mu}_j$, and $\boldsymbol{L}_j$, by viewing an iteration process as an Euler discretization of an ODE [41, 42, 43]. $\boldsymbol{\Sigma}_j$ is computed by $\boldsymbol{\Sigma}_j = \boldsymbol{L}_j\boldsymbol{L}_j^\top$. Concretely, we denote the distribution parameter as ξ (it can be c, $\boldsymbol{\mu}_j$, or

$\boldsymbol{L}_j$) and the estimation of ξ can be cast as an iterative optimization process using given data (*e.g.*, maximizing the likelihood), $\xi^{t+1} = \xi^t + \nabla\xi^t$, where $\nabla\xi^t$ is the gradient at step t. We regard the iterative optimization process as a continues-time process of an ODE, and propose a gradient flow network F to estimate the gradient flow $\frac{d\xi^t}{dt}$ at time t, $\nabla\xi^t = \frac{d\xi^t}{dt} = F(\xi^t, t)$. Thus, given the initial value ξ^0 and F, the distribution parameter is obtained by solving the ODE at the last time T with an integral term: $\xi^T = \xi^0 + \int_{t=0}^{T} F(\xi^t, t)dt$.

Here, we utilize the Runge-Kutta method [44] denoted by $\mathrm{ODESolve}(\cdot)$ to solve the integral term,

$$\xi^T = \mathrm{ODESolve}(\xi^0, F, T). \tag{7}$$

In implementation, we use three gradient flow networks F_1, F_2, and F_3 to produce the gradient flow for c, $\boldsymbol{\mu}_j$, and $\boldsymbol{L}_j$, respectively. ξ^0 for $\boldsymbol{\mu}_j$ and $\boldsymbol{L}_j$ is obtained by computing the mean of given data and subtracting the mean from given data, and ξ^0 for c is set as a fixed value.

Gradient flow network. This network takes the distribution parameter ξ^t and features of a set of samples as inputs, and generates the gradient $\frac{d\xi^t}{dt}$ via three layers, as shown in Figure 2. We first build an estimation representation $\boldsymbol{e}_j$ for each class, where ξ^t and the mean $\overline{\boldsymbol{x}}_j$ of features belonging to the j-th class are concatenated as $\boldsymbol{e}_j = [\xi^t, \overline{\boldsymbol{x}}_j]$.

We use a fully-connected layer f_e to embed $\boldsymbol{e}_j$ as

$$\boldsymbol{e}'_j = f_e(\boldsymbol{e}_j). \tag{8}$$

Then, we use a self-attention layer f_t to perform interaction among different classes,

$$\boldsymbol{e}''_j = f_t\left(\{\boldsymbol{e}'_j\}_{j=1}^n\right). \tag{9}$$

where the query, key, and value of the self-attention layer are all $\{\boldsymbol{e}'_j\}_{j=1}^n$ of classes, with n classes in total. Finally, we use a fully-connected layer f_o to create the gradient,

$$\frac{d\xi^t}{dt} = f_o(\{\boldsymbol{e}''_j\}). \tag{10}$$

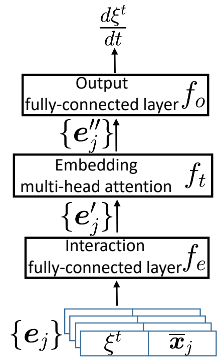

$\frac{d\xi^t}{dt}$
Output fully-connected layer f_o
$\{\boldsymbol{e}''_j\}$
Embedding multi-head attention f_t
$\{\boldsymbol{e}'_j\}$
Interaction fully-connected layer f_e
$\{\boldsymbol{e}_j\}$
ξ^t
$\overline{\boldsymbol{x}}_j$

Figure 2: Architecture of the gradient flow network.

Note that, we employ a common curvature c for all classes using F_1, instead of producing class-specific curvatures and unifying them. We send all data of the n classes together to the gradient flow network F_1, concatenate the representation of all classes $\{\boldsymbol{e}''_j\}_{j=1}^n$, and use the output fully-connected layer f_o to produce the gradient flow for the common curvature c.

4.4 Learning with Infinite Data Augmentation

We use a distance-based classifier in the hyperbolic space, and a feature is classified by assigning it to the closest weight of classes. We represent the weight of the j-th class as $\boldsymbol{w}_j \in \mathcal{M}^{d,c}$, and the classifier is denoted by $\boldsymbol{W} = [\boldsymbol{w}_1, \cdots, \boldsymbol{w}_n]$. The probability that a hyperbolic feature $\boldsymbol{x}$ belongs to the j-th class is

$$p(\widehat{y} = j|\boldsymbol{x}) = \frac{\exp\big(-d^c(\boldsymbol{x}, \boldsymbol{w}_j)\big)}{\sum_{j'=1}^{n}\exp\big(-d^c(\boldsymbol{x}, \boldsymbol{w}_{j'})\big)}, \tag{11}$$

where $\widehat{y}$ is the prediction of the classifier.

We sample features from the estimated distribution to train the classifier. We denote the augmented features for the j-th class by $\{\boldsymbol{z}_{j,i}\}_{i=1}^m$, where $\boldsymbol{z}_{j,i} \sim \mathcal{P}(c, \boldsymbol{p}_j, \boldsymbol{\mu}_j, \boldsymbol{\Sigma}_j)$ (a total of m samples are generated per class). The classifier is trained by minimizing the following cross-entropy loss function,

$$\mathcal{L}(\boldsymbol{W}) = \frac{1}{n}\sum_{j=1}^{n}\frac{1}{m}\sum_{i=1}^{m} -\log\frac{\exp\big(-d^c(\boldsymbol{z}_{j,i}, \boldsymbol{w}_j)\big)}{\sum_{j'=1}^{n}\exp\big(-d^c(\boldsymbol{z}_{j,i}, \boldsymbol{w}_{j'})\big)}. \tag{12}$$

A large value of m brings more diversity to the model, promising the model to learn the invariance of each class. Considering m grows to infinity, the loss function is defined by the expectation of the cross-entropy,

$$\mathcal{L}_\infty(\boldsymbol{W}) = \frac{1}{n}\sum_{j=1}^{n}\mathbb{E}_i\left[-\log\frac{\exp\big(-d^c(\boldsymbol{z}_{j,i}, \boldsymbol{w}_j)\big)}{\sum_{j'=1}^{n}\exp\big(-d^c(\boldsymbol{z}_{j,i}, \boldsymbol{w}_{j'})\big)}\right]. \tag{13}$$

Computing Eq. (13) is difficult and the computational load of if MCMC methods are used for a large value of m. Alternatively, we derive an upper bound $\overline{\mathcal{L}}_\infty(\boldsymbol{W})$ of $\mathcal{L}_\infty(\boldsymbol{W})$, which is easy to compute, as shown in Proposition 1. In this case, we train the classifier by minimizing the upper bound $\overline{\mathcal{L}}_\infty(\boldsymbol{W})$, rather than the original loss function $\mathcal{L}_\infty(\boldsymbol{W})$.

Proposition 1. *Given infinite data $\boldsymbol{z}_{j,i} \sim \mathcal{P}(c, \boldsymbol{p}_j, \boldsymbol{\mu}_j, \boldsymbol{\Sigma}_j)$, an upper bound of the loss function $\mathcal{L}_\infty$ in Eq.* (13) *is given by*

$$\overline{\mathcal{L}}_\infty(\boldsymbol{W}) = \frac{1}{n}\sum\nolimits_{j=1}^{n} -\log \frac{\exp\left(\boldsymbol{w}_j^\top(\widehat{\boldsymbol{p}}_j + \boldsymbol{\mu}_i)\right)}{\sum_{j'=1}^{n}\exp\left(\boldsymbol{w}_{j'}^\top(\widehat{\boldsymbol{p}}_j + \boldsymbol{\mu}_i) + (\boldsymbol{w}_{j'}^\top\boldsymbol{w}_{j'} - \boldsymbol{w}_j^\top\boldsymbol{w}_j) + \frac{1}{2}(\boldsymbol{w}_{j'} - \boldsymbol{w}_j)^\top\boldsymbol{\Sigma}_j(\boldsymbol{w}_{j'} - \boldsymbol{w}_j)\right)}, \tag{14}$$

where $\boldsymbol{p}_j = \mathrm{expm}_{\boldsymbol{0}}^{c}(\widehat{\boldsymbol{p}}_j)$, and $\widehat{\boldsymbol{p}}_j$ can be directly computed in the tangent space at the origin.

Proof. We rewrite the loss function of the infinite data augmentation in Eq. (13) as

$$\mathcal{L}_\infty(\boldsymbol{W}) = \frac{1}{n}\sum_{j=1}^{n}\mathbb{E}_i\left[-\log\left(\frac{\exp\Big(-d^c(\boldsymbol{z}_{j,i},\boldsymbol{w}_j)\Big)}{\sum_{j'=1}^{n}\exp\Big(-d^c(\boldsymbol{z}_{j,i},\boldsymbol{w}_{j'})\Big)}\right)\right]$$

$$=\frac{1}{n}\sum_{j=1}^{n}\mathbb{E}_i\left[\log\left(\sum_{j'=1}^{n}\exp\Big(d^c(\boldsymbol{z}_{j,i},\boldsymbol{w}_j) - d^c(\boldsymbol{z}_{j,i},\boldsymbol{w}_{j'})\Big)\right)\right]$$

$$\leq\frac{1}{n}\sum_{j=1}^{n}\log\Big(\sum_{j'=1}^{n}\mathbb{E}_i\left[\exp\left(d^c(\boldsymbol{z}_{j,i},\boldsymbol{w}_j) - d^c(\boldsymbol{z}_{j,i},\boldsymbol{w}_{j'})\right)\right]\Big) \tag{15a}$$

$$\leq\frac{1}{n}\sum_{j=1}^{n}\log\Big(\sum_{j'=1}^{n}\mathbb{E}_i\left[\exp\left(\|\boldsymbol{z}_{j,i} - \boldsymbol{w}_j\|^2 - \|\boldsymbol{z}_{j,i} - \boldsymbol{w}_{j'}\|^2\right)\right]\Big) \tag{15b}$$

$$=\frac{1}{n}\sum_{j=1}^{n}\log\Big(\sum_{j'=1}^{n}\mathbb{E}_i\left[\exp\left(2(\boldsymbol{w}_{j'} - \boldsymbol{w}_j)^\top\boldsymbol{z}_{j,i} + (\boldsymbol{w}_{j'}^\top\boldsymbol{w}_{j'} - \boldsymbol{w}_j^\top\boldsymbol{w}_j)\right)\right]\Big)$$

$$\leq\frac{1}{n}\sum_{j=1}^{n}\log\left(\sum_{j'=1}^{n}\mathbb{E}_i\left[\exp\left((\boldsymbol{w}_{j'} - \boldsymbol{w}_j)^\top(\widehat{\boldsymbol{p}}_j + \widehat{\boldsymbol{v}}_{j,i}) + (\boldsymbol{w}_{j'}^\top\boldsymbol{w}_{j'} - \boldsymbol{w}_j^\top\boldsymbol{w}_j)\right)\right]\right) \tag{15c}$$

$$=\frac{1}{n}\sum_{j=1}^{n}\log\left(\sum_{j'=1}^{n}\exp\Big((\boldsymbol{w}_{j'} - \boldsymbol{w}_j)^\top(\widehat{\boldsymbol{p}}_j + \boldsymbol{\mu}_j) + (\boldsymbol{w}_{j'}^\top\boldsymbol{w}_{j'} - \boldsymbol{w}_j^\top\boldsymbol{w}_j) + \frac{1}{2}(\boldsymbol{w}_{j'} - \boldsymbol{w}_j)^\top\boldsymbol{\Sigma}_j(\boldsymbol{w}_{j'} - \boldsymbol{w}_j)\Big)\right) \tag{15d}$$

$$=\frac{1}{n}\sum_{j=1}^{n} -\log\frac{\exp\left(\boldsymbol{w}_j(\widehat{\boldsymbol{p}}_j + \boldsymbol{\mu}_j)\right)}{\exp\left(\boldsymbol{w}_{j'}(\widehat{\boldsymbol{p}}_j + \boldsymbol{\mu}_j) + (\boldsymbol{w}_{j'}^\top\boldsymbol{w}_{j'} - \boldsymbol{w}_j^\top\boldsymbol{w}_j) + \frac{1}{2}(\boldsymbol{w}_{j'} - \boldsymbol{w}_j)^\top\boldsymbol{\Sigma}_j(\boldsymbol{w}_{j'} - \boldsymbol{w}_j)\right)}$$

$$=\overline{\mathcal{L}}_\infty(\boldsymbol{W}).$$

Eq. (15a) follows from the Jensen's inequality $\mathbb{E}[\log(\boldsymbol{x})] \leq \log\mathbb{E}[\boldsymbol{x}]$. For Eq. (15b), we define a function $f = d^c(\boldsymbol{x},\boldsymbol{y}) - \|\boldsymbol{x} - \boldsymbol{y}\|^2$ and compute the derivative of f. We find f is an increasing function when $\|\boldsymbol{x} - \boldsymbol{y}\|^2 < \frac{\sqrt{1+|c|}-\sqrt{|c|}}{\sqrt{|c|}}$. In this case, if we have $\|\boldsymbol{z}_{j,i} - \boldsymbol{w}_j\|^2 < \|\boldsymbol{z}_{j,i} - \boldsymbol{w}_{j'}\|^2 < \frac{\sqrt{1+|c|}-\sqrt{|c|}}{\sqrt{|c|}}$, we can derive $d^c(\boldsymbol{z}_{j,i},\boldsymbol{w}_j) - \|\boldsymbol{z}_{j,i},\boldsymbol{w}_j\|^2 < d^c(\boldsymbol{z}_{j,i},\boldsymbol{w}_{j'}) - \|\boldsymbol{z}_{j,i},\boldsymbol{w}_{j'}\|^2$ and $\|\boldsymbol{z}_{j,i},\boldsymbol{w}_j\|^2 - \|\boldsymbol{z}_{j,i},\boldsymbol{w}_{j'}\|^2 > d^c(\boldsymbol{z}_{j,i},\boldsymbol{w}_j) - d^c(\boldsymbol{z}_{j,i},\boldsymbol{w}_{j'})$. Eq. (15c) is obtained by replacing $\boldsymbol{z}_{j,i}$ with the augmentation process using the parallel transport and exponential map, *i.e.*, $\boldsymbol{z}_{j,i} = \mathrm{expm}_{\boldsymbol{p}_j}^{c}(\mathrm{PT}_{\boldsymbol{0}\to\boldsymbol{p}_j}^{c}(\widehat{\boldsymbol{v}}_{j,i}))$, and adding scale constraints on c, $\|\widehat{\boldsymbol{v}}_{j,i}\|$, and $\|\widehat{\boldsymbol{p}}_j\|$. Eq. (15d) is obtained by using the moment-generating function: $\mathbb{E}[\exp(\boldsymbol{x})] = \exp(\boldsymbol{\mu} + \frac{1}{2}\boldsymbol{\Sigma})$, $\boldsymbol{x} \sim \mathcal{N}(\boldsymbol{\mu},\boldsymbol{\Sigma})$. In our derivation, $(\boldsymbol{w}_{j'} - \boldsymbol{w}_j)^\top(\widehat{\boldsymbol{p}}_j + \widehat{\boldsymbol{v}}_{j,i}) + (\boldsymbol{w}_{j'}^\top\boldsymbol{w}_{j'} - \boldsymbol{w}_j^\top\boldsymbol{w}_j)$ is a Gaussian vector. □

Detailed derivation and implementation can be found in the supplementary materials. From this derivation, we replace a non-Euclidean loss function with a Euclidean upper bound by adding suitable constraints. The upper bound is easy to compute without explicit augmentation and time-consumption hyperbolic operations, and our experimental results show that it achieves good performance (see

Section 5). This provides an interesting research direction and feasible way for Riemannian algorithms whose loss functions are difficult or high-cost to compute.

The classifier $\boldsymbol{W}$ is updated by the Riemannian gradient descent algorithm [45] in the process of minimizing $\overline{\mathcal{L}}_\infty(\boldsymbol{W})$. After several iterations, we obtain the updated classifier $\boldsymbol{W}^* = [\boldsymbol{w}_1^*, \cdots, \boldsymbol{w}_n^*]$, and test data is classified by Eq. (11).

4.5 Training

The goal of this work is to learn the gradient flow networks F_1, F_2, and F_3. In doing so, we train them in a meta-learning framework that simulates the practical setting by using some base data $\mathcal{D}$. In the training stage, we randomly select few data from $\mathcal{D}$ as the training data $\mathcal{D}_t$, and the rest is used as the validation data $\mathcal{D}_v$. F_1, F_2, and F_3 are updated via a bi-level optimization manner. In the inner-loop, we estimate the distribution of $\mathcal{D}_t$ by using F_1, F_2, and F_3, iteratively train the classifier $\boldsymbol{W}$ by minimizing the loss function $\overline{\mathcal{L}}_\infty$, and obtain the updated classifier $\boldsymbol{W}^* = [\boldsymbol{w}_1^*, \cdots, \boldsymbol{w}_n^*]$. We update F_1, F_2, and F_3 in the outer-loop by minimizing the following objective that is the loss of $\boldsymbol{W}^*$ on the validation data $\mathcal{D}_v$,

$$\begin{aligned}\min_{F_1,F_2,F_3} \mathcal{L}(\boldsymbol{W}^*) = & \mathbb{E}_{\boldsymbol{x}\sim\mathcal{D}_v}\left[-\sum_{j=1}^{n} \mathbb{1}_{y=j} \log \frac{\exp\big(-d^c(\boldsymbol{x}, \boldsymbol{w}_j^*)\big)}{\sum_{j'=1}^{n}\exp\big(-d^c(\boldsymbol{x}, \boldsymbol{w}_{j'}^*)\big)}\right], \\ & \text{s.t. } \boldsymbol{W}^* = \arg\min_{\boldsymbol{W}} \overline{\mathcal{L}}_\infty(\boldsymbol{W})\end{aligned} \quad (16)$$

where $\mathbb{1}_{y=j}$ is the indicator function, meaning that if the label y of $\boldsymbol{x}$ is equal to j, $\mathbb{1}_{y=j} = 1$, and 0 otherwise. The pseudo code of training is summarized in Algorithm 2.

In the inference stage, given a task with limited data, our method first estimates the distribution for each class by using the learned F_1, F_2, and F_3, and then trains the model by using $\overline{\mathcal{L}}_\infty$.

Algorithm 2 Training process of HFA.

```
Input: Base data $\mathcal{D}$.
Output: Updated gradient flow networks $F_1$, $F_2$, $F_3$.
1: while Not converged do
2:     Randomly select few training data $\mathcal{D}_t$ from $\mathcal{D}$,
       and the rest of $\mathcal{D}$ is used as validation data $\mathcal{D}_v$.
3:     Estimate the distribution for each class in $\mathcal{D}_t$ by
       using $F_1$, $F_2$, and $F_3$ via Eq. (7).
4:     while Not converged do
5:         Train the classifier $\boldsymbol{W}$ using the estimated dis-
           tribution via the loss function in Eq. (14).
6:     end while
7:     Compute the loss of the updated classifier $\boldsymbol{W}^*$
       using the validation data $\mathcal{D}_v$, and update $F_1$, $F_2$,
       and $F_3$ via minimizing Eq. (16).
8: end while
```

5 Experiments

We evaluate the proposed method HFA on few-shot learning and continual learning tasks. In few-shot learning, data augmentation is a natural idea to overcome the deficiency of training data [25, 26]. In continual learning, reply-based methods have shown effectiveness in continual learning by storing data [46, 47], yet they cannot store much data due to the memory limitation. We use HFA to perform augmentation for stored limited data to solve this issue. We use common backbone networks with exponential map as the feature extractor in the two tasks. More experiments (*e.g.*, evaluation on graph data, visualization, and ablation) and experimental details can be found in the supplementary materials.

5.1 Few-shot Learning

We conducted experiments on four few-shot learning datasets: mini-ImageNet [48], tiered-ImageNet [49], CUB [7], and CIFAR-FS [50] datasets. The four datasets have hyperbolic structures, and are commonly used to evaluate hyperbolic algorithms [3, 9, 29, 28]. We use ResNet12 and ResNet18 as the backbone networks, and perform augmentation for the support data.

5.1.1 Main Results

We compare HFA with augmentation-based few-shot learning methods [22, 51, 25, 26, 52, 53, 54, 55, 27] on the mini-ImageNet, CUB, and CIFAR-FS datasets. These methods all augment data in Euclidean space, while HFA performs data augmentation in the hyperbolic space. Our method brings improvements on them, as shown in Table 1. In particular, VFSL [54] and V1-Net [25] study data

Table 1: Accuracy (%) comparisons with Euclidean augmentation-based few-shot learning methods on the mini-ImageNet, CUB, and CIFAR-FS datasets.

Method	**Backbone**	**mini-ImageNet**		**CUB**		**CIFAR-FS**	
		1-shot	5-shot	1-shot	5-shot	1-shot	5-shot
VFSL [54]	ResNet12	61.23 ± 0.26	77.69 ± 0.17	-	-	-	-
DTN [55]	ResNet12	63.45 ± 0.86	77.91 ± 0.62	72.00	85.10	71.50	82.80
Ours	ResNet12	$\mathbf{66.87 \pm 0.44}$	$\mathbf{82.08 \pm 0.31}$	$\mathbf{76.75 \pm 0.43}$	$\mathbf{89.19 \pm 0.26}$	$\mathbf{72.52 \pm 0.46}$	$\mathbf{85.33 \pm 0.33}$
Delta-encoder [52]	VGG-16	59.9	69.7	69.80 ± 0.46	82.60 ± 0.35	66.70	79.80
SalNet [53]	ResNet101	62.22 ± 0.87	77.95 ± 0.65	-	-	-	-
Dual TriNet [22]	ResNet18	58.12 ± 1.37	76.92 ± 0.69	69.61	84.10	63.41 ± 0.64	78.43 ± 0.64
IDeMe-Net [51]	ResNet18	59.14 ± 0.86	74.63 ± 0.74	-	-	-	-
V1-Net [25]	ResNet18	61.05	78.60	74.76	86.84	-	-
AFHN [26]	ResNet18	62.38 ± 0.72	78.16 ± 0.56	70.53 ± 1.01	83.95 ± 0.63	68.32 ± 0.93	81.45 ± 0.87
TFH [27]	ResNet18	65.07 ± 0.82	80.81 ± 0.61	75.76 ± 0.83	88.60 ± 0.47	74.77 ± 0.90	86.88 ± 0.59
HFA (Ours)	ResNet18	$\mathbf{68.26 \pm 0.46}$	$\mathbf{83.53 \pm 0.28}$	$\mathbf{77.25 \pm 0.45}$	$\mathbf{90.77 \pm 0.26}$	$\mathbf{75.08 \pm 0.47}$	$\mathbf{87.24 \pm 0.33}$

Table 2: Accuracy (%) comparisons with popular few-shot learning methods on the mini-ImageNet and tiered-ImageNet datasets. 'Optim', 'Metric', and 'Aug' denote the optimization-based, metric-based, and augmentation-based few-shot learning methods, respectively. 'Euclidean' and 'Hyperbolic' denote the algorithm is in Euclidean space and hyperbolic space, respectively. $\star$ means that HyperProto uses ResNet18 as the backbone, while the others use ResNet12.

Method	**Category**	**mini-ImageNet**		**tiered-ImageNet**	
		1-shot	5-shot	1-shot	5-shot
MAML [56]	Euclidean Optim	51.03 ± 0.50	68.26 ± 0.47	58.58 ± 0.49	71.24 ± 0.43
L2F [57]	Euclidean Optim	57.48 ± 0.49	74.68 ± 0.43	63.94 ± 0.84	77.61 ± 0.41
ALFA [58]	Euclidean Optim	60.06 ± 0.49	77.42 ± 0.42	64.43 ± 0.49	81.77 ± 0.39
MeTAL [59]	Euclidean Optim	59.64 ± 0.38	76.20 ± 0.19	63.89 ± 0.43	80.14 ± 0.40
CurAML [9]	Hyperbolic Optim	63.13 ± 0.41	81.04 ± 0.39	68.46 ± 0.56	83.84 ± 0.40
ProtoNet [60]	Euclidean Metric	56.52 ± 0.45	74.28 ± 0.20	53.51 ± 0.89	72.69 ± 0.74
MetaOptNet [61]	Euclidean Metric	62.64 ± 0.61	78.63 ± 0.46	65.99 ± 0.72	81.56 ± 0.53
DSN [62]	Euclidean Metric	62.64 ± 0.66	78.83 ± 0.45	66.22 ± 0.75	82.79 ± 0.48
FEAT [8]	Euclidean Metric	66.78 ± 0.20	82.05 ± 0.14	70.80 ± 0.23	84.79 ± 0.16
HyperProto* [3]	Hyperbolic Metric	59.47 ± 0.20	76.84 ± 0.14	-	-
w/o Aug	Hyperbolic -	64.75 ± 0.35	79.84 ± 0.20	68.57 ± 0.49	82.22 ± 0.39
Inf Aug	Hyperbolic Aug	65.12 ± 0.45	80.78 ± 0.32	70.22 ± 0.50	84.51 ± 0.37
Neural ODE + Aug 5 samples	Hyperbolic Aug	65.54 ± 0.46	80.96 ± 0.31	69.32 ± 0.53	83.21 ± 0.35
HFA (Ours) (Neural ODE + Inf Aug)	Hyperbolic Aug	$\mathbf{66.87 \pm 0.44}$	$\mathbf{82.08 \pm 0.31}$	$\mathbf{71.62 \pm 0.49}$	$\mathbf{85.47 \pm 0.35}$

augmentation in the Euclidean feature space, while our method has better performance. For example, on the mini-ImageNet dataset using ResNet12, our method improves VFSL by 5.64% and 4.39% in the 1-shot and 5-shot tasks, respectively. The main reason is that augmentation in the hyperbolic space preserves the hierarchical structures of data and avoids the undesirable data distortion. Results on Resnet18 indicate the superiority of our method again, demonstrating the significance of data augmentation in the hyperbolic space.

We then compare HFA with popular optimization-based and metric-based few-shot learning methods on the mini-ImageNet and tiered-ImageNet datasets. Results are shown in Table 2. L2F [57], ALFA [58], MeTAL [59], and CurAML [9] are state-of-the-art optimization-based methods. Similar to them, the adaptation to new tasks of HFA is also achieved by an optimization process. Our method improves them by 3% on the 1-shot task and $1\% - 2\%$ on the 5-shot task. Compared with metric-based methods, including HyperProto [3], MetaOptNet [61], DSN [62], and FEAT [8], Our method performs competitively or even exceeds some methods. Note that CurAML and HyperProto are both few-shot learning methods in the hyperbolic space, and our better performance suggests that our data augmentation can actually improve the model in scarce data regimes.

5.1.2 Ablation

We conduct ablation experiments to show effectiveness of our neural ODE and the derived upper bound of the augmentation loss. We first denote 'not performing any augmentation' as 'w/o aug', where we directly use the given data to train the classifier. Then, we perform infinite augmentation, where the curvature is tuned manually, and the mean and covariance matrix are directly computed from the given data, denoted by 'Inf Aug'. Next, we use the neural ODE to estimate the distribution, and generate 5 samples for each class, denoted by 'Neural ODE + Aug 5 samples'. Finally, based on the estimated distribution, we perform infinite augmentation, denoted by 'Neural ODE + Inf Aug'. Results are shown in Table 2. We find that 'Inf Aug' has better performance than 'w/o aug',

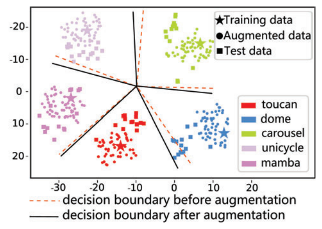

(a) Feature distribution.

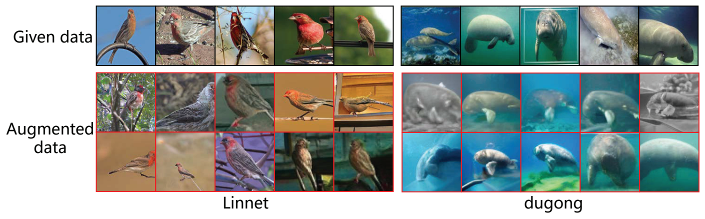

(b) Corresponding images of generated features.

Figure 3: Visualization of augmentation data.

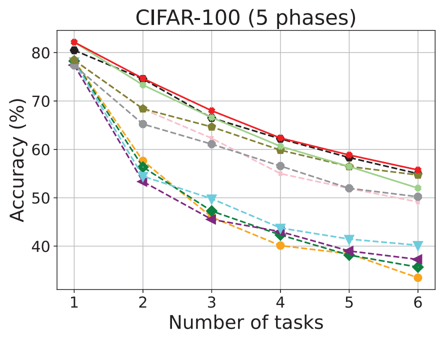

(a) 5-phases

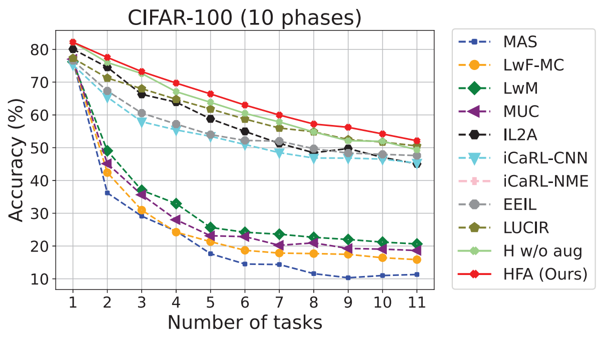

(b) 10-phases

Figure 4: Top-1 accuracy on CIFAR-100 in continual learning.

showing that the infinite augmentation improves the generalization ability in the hyperbolic space. Using neural ODE further improves the performance on the two datasets. The reason is that directly computing the mean and covariance matrix from limited data results in imprecise distributions. In contrast, our neural ODE makes a better approximation to the real distribution.

5.1.3 Visualization

We first plot the estimated distribution in mini-ImageNet by sampling augmented features, where the MDS and t-SNE dimensionality reduction methods are used. Then, we use a reverse mapping algorithm [12] to search images corresponding to the augmented features for intuitive visualization. Results are shown in Figure 3. In the left panel, when training data is biased, our method well approximates the real distribution, building a robust decision boundary for classification. In the right panel, generated data has much diversities (*e.g.*, background and object posture) while preserving the class-identity.

5.2 Continual Learning

We use the CIFAR-100 dataset [50] with 100 classes. We evaluate HFA on two settings: $50 + 5 \times 10$ and $50 + 10 \times 5$. For example, $50 + 5 \times 10$ means that the first task contains 50 classes, and there are 10 following tasks with each one having 5 classes. We use ResNet18 as the backbone, and the model is updated by a cross-entropy loss on current data, an infinite augmentation loss on stored data, and a distillation loss. HFA stores 20 samples for each class, which is the same as replay-based methods [63, 64, 65]. Comparisons with MAS [66], LwF-MC [63], LwM [67], MUC [68], IL2A [69], iCaRL [63], EEIL [64], and LUCIR [65] are shown in Figure 4. Meanwhile, an ablation experiment where augmentation is not performed is denoted by 'H w/o aug'. Our method has better performance than replay based methods [63, 64, 65]. The reason is that our method is capable of estimating the distribution from few data, and thus leads to diverse and discriminative augmentation for stored data, making the model more reliable. In addition, our method performs better than the augmentation-based method IL2A [69]. This suggests that modeling data in the hyperbolic space is more discriminative, and performing augmentation in the hyperbolic space can further leads to a robust model.

6 Conclusions

In this paper, we have presented a hyperbolic feature augmentation (HFA) method that generates diverse and discriminative features to overcome overfitting in the hyperbolic space. The introduced meta-neural-ODE distribution estimation scheme can precisely approximate the real distribution in scarce data regimes. The derived upper bound of the augmentation loss makes an efficient augmentation algorithm in the hyperbolic space, which not only leads to much diversity of data but also reduces much computational load. Experiments in few-shot learning and continual learning tasks show that our method can improve the generalization of hyperbolic algorithms in scarce data regimes. In this work, we assume that data has a uniform hierarchical structure and use a single hyperbolic space for each task. Actually, real-world data may have complex hierarchical structures with varying local structures. In the future, we will study data augmentation in product manifolds to tackle such complex data.

Acknowledgements. This work was supported by the Natural Science Foundation of China (NSFC) under Grants No. 62172041 and No. 62176021.

References

[1] Wei Peng, Tuomas Varanka, Abdelrahman Mostafa, Henglin Shi, and Guoying Zhao. Hyperbolic deep neural networks: A survey. *IEEE Transactions on Pattern Analysis and Machine Intelligence (T-PAMI)*, 2021. doi:10.1109/TPAMI.2021.3136921.

[2] Pengfei Fang, Mehrtash Harandi, and Lars Petersson. Kernel methods in hyperbolic spaces. In *IEEE/CVF International Conference on Computer Vision (ICCV)*, pages 10665–10674, 2021.

[3] Valentin Khrulkov, Leyla Mirvakhabova, Evgeniya Ustinova, Ivan V. Oseledets, and Victor S. Lempitsky. Hyperbolic image embeddings. In *IEEE/CVF Conference on Computer Vision and Pattern Recognition (CVPR)*, pages 6417–6427, 2020.

[4] Teng Long, Pascal Mettes, Heng Tao Shen, and Cees G. M. Snoek. Searching for actions on the hyperbole. In *IEEE/CVF Conference on Computer Vision and Pattern Recognition (CVPR)*, pages 1138–1147, 2020.

[5] Jindou Dai, Yuwei Wu, Zhi Gao, and Yunde Jia. A hyperbolic-to-hyperbolic graph convolutional network. In *IEEE/CVF Conference on Computer Vision and Pattern Recognition (CVPR)*, pages 154–163, 2021.

[6] Ryohei Shimizu, Yusuke Mukuta, and Tatsuya Harada. Hyperbolic neural networks++. In *International Conference on Learning Representations (ICLR)*, 2021.

[7] Catherine Wah, Steve Branson, Peter Welinder, Pietro Perona, and Serge Belongie. The caltech-ucsd birds-200-2011 dataset. 2011.

[8] Han-Jia Ye, Hexiang Hu, De-Chuan Zhan, and Fei Sha. Few-shot learning via embedding adaptation with set-to-set functions. In *IEEE/CVF Conference on Computer Vision and Pattern Recognition (CVPR)*, pages 8808–8817, 2020.

[9] Zhi Gao, Yuwei Wu, Mehrtash T Harandi, and Yunde Jia. Curvature-adaptive meta-learning for fast adaptation to manifold data. *IEEE Transactions on Pattern Analysis and Machine Intelligence (T-PAMI)*, 2022. doi:10.1109/TPAMI.2022.3164894.

[10] Pan Li, Da Li, Wei Li, Shaogang Gong, Yanwei Fu, and Timothy M. Hospedales. A simple feature augmentation for domain generalization. In *IEEE/CVF International Conference on Computer Vision (ICCV)*, pages 8866–8875, 2021.

[11] Yuhang Zang, Chen Huang, and Chen Change Loy. FASA: feature augmentation and sampling adaptation for long-tailed instance segmentation. In *IEEE/CVF International Conference on Computer Vision (ICCV)*, pages 3437–3446, 2021.

[12] Yulin Wang, Xuran Pan, Shiji Song, Hong Zhang, Gao Huang, and Cheng Wu. Implicit semantic data augmentation for deep networks. In *Neural Information Processing Systems (NeurIPS)*, pages 12614–12623, 2019.

[13] Shuang Li, Kaixiong Gong, Chi Harold Liu, Yulin Wang, Feng Qiao, and Xinjing Cheng. Metasaug: Meta semantic augmentation for long-tailed visual recognition. In *IEEE/CVF Conference on Computer Vision and Pattern Recognition (CVPR)*, pages 5212–5221, 2021.

[14] Karen Simonyan and Andrew Zisserman. Very deep convolutional networks for large-scale image recognition. In *International Conference on Learning Representations (ICLR)*, 2015.

[15] Chengyue Gong, Dilin Wang, Meng Li, Vikas Chandra, and Qiang Liu. Keepaugment: A simple information-preserving data augmentation approach. *IEEE/CVF Conference on Computer Vision and Pattern Recognition (CVPR)*, pages 1055–1064, 2021.

[16] Denis A. Gudovskiy, L. Rigazio, Shun Ishizaka, Kazuki Kozuka, and Sotaro Tsukizawa. Autodo: Robust autoaugment for biased data with label noise via scalable probabilistic implicit differentiation. *IEEE/CVF Conference on Computer Vision and Pattern Recognition (CVPR)*, pages 16596–16605, 2021.

[17] Sungbin Lim, Ildoo Kim, Taesup Kim, Chiheon Kim, and Sungwoong Kim. Fast autoaugment. In *Neural Information Processing Systems (NeurIPS)*, pages 6662–6672, 2019.

[18] Liming Jiang, Bo Dai, Wayne Wu, and Chen Change Loy. Deceive D: Adaptive Pseudo Augmentation for GAN training with limited data. In *Neural Information Processing Systems (NeurIPS)*, pages 21655–21667, 2021.

[19] Liming Jiang, Bo Dai, Wayne Wu, and Chen Change Loy. Deceive d: Adaptive pseudo augmentation for gan training with limited data. In *Neural Information Processing Systems (NeurIPS)*, pages 21655–21667, 2021.

[20] Qi Cai, Yu Wang, Yingwei Pan, Ting Yao, and Tao Mei. Joint contrastive learning with infinite possibilities. In *Neural Information Processing Systems (NeurIPS)*, pages 12638–12648, 2020.

[21] Shuang Li, Mixue Xie, Kaixiong Gong, Chi Harold Liu, Yulin Wang, and Wei Li. Transferable semantic augmentation for domain adaptation. In *IEEE/CVF Conference on Computer Vision and Pattern Recognition (CVPR)*, pages 11516–11525, 2021.

[22] Zitian Chen, Yanwei Fu, Yinda Zhang, Yu-Gang Jiang, Xiangyang Xue, and Leonid Sigal. Multi-level semantic feature augmentation for one-shot learning. *IEEE Transactions on Image Processing (T-IP)*, 28(9):4594–4605, 2019.

[23] Vikas Verma, Alex Lamb, Christopher Beckham, Amir Najafi, Ioannis Mitliagkas, David Lopez-Paz, and Yoshua Bengio. Manifold mixup: Better representations by interpolating hidden states. In *International Conference on Machine Learning (ICML)*, pages 6438–6447, 2019.

[24] Boyi Li, Felix Wu, Ser-Nam Lim, Serge J. Belongie, and Kilian Q. Weinberger. On feature normalization and data augmentation. In *IEEE/CVF Conference on Computer Vision and Pattern Recognition (CVPR)*, pages 12378–12387, 2021.

[25] Qinxuan Luo, Lingfeng Wang, Jingguo Lv, Shiming Xiang, and Chunhong Pan. Few-shot learning via feature hallucination with variational inference. In *IEEE/CVF Winter Conference on Applications of Computer Vision (WACV)*, pages 3962–3971, 2021.

[26] Kai Li, Yulun Zhang, Kunpeng Li, and Yun Fu. Adversarial feature hallucination networks for few-shot learning. In *IEEE/CVF Conference on Computer Vision and Pattern Recognition (CVPR)*, pages 13467–13476, 2020.

[27] Michalis Lazarou, Yannis Avrithis, and Tania Stathaki. Tensor feature hallucination for few-shot learning. In *IEEE/CVF Winter Conference on Applications of Computer Vision (WACV)*, pages 2050–2060, 2022.

[28] Zhi Gao, Yuwei Wu, Yunde Jia, and Mehrtash Harandi. Curvature generation in curved spaces for few-shot learning. In *IEEE/CVF International Conference on Computer Vision (ICCV)*, pages 8671–8680, 2021.

[29] Jiexi Yan, Lei Luo, Cheng Deng, and Heng Huang. Unsupervised hyperbolic metric learning. In *IEEE/CVF Conference on Computer Vision and Pattern Recognition (CVPR)*, pages 12465–12474, 2021.

[30] Mina Ghadimi Atigh, Julian Schoep, Erman Acar, Nanne van Noord, and Pascal Mettes. Hyperbolic image segmentation. In *IEEE/CVF Conference on Computer Vision and Pattern Recognition (CVPR)*, pages 4443–4452, 2022.

[31] Qi Liu, Maximilian Nickel, and Douwe Kiela. Hyperbolic graph neural networks. In *Neural Information Processing Systems (NeurIPS)*, pages 8230–8241, 2019.

[32] Çaglar Gülçehre, Misha Denil, Mateusz Malinowski, Ali Razavi, Razvan Pascanu, Karl Moritz Hermann, Peter W. Battaglia, Victor Bapst, David Raposo, Adam Santoro, and Nando de Freitas. Hyperbolic attention networks. In *International Conference on Learning Representations (ICLR)*, 2019.

[33] Ondrej Skopek, Octavian-Eugen Ganea, and Gary Bécigneul. Mixed-curvature variational autoencoders. In *International Conference on Learning Representations (ICLR)*, 2020.

[34] Emile Mathieu, Charline Le Lan, Chris J. Maddison, Ryota Tomioka, and Yee Whye Teh. Continuous hierarchical representations with poincaré variational auto-encoders. In *Neural Information Processing Systems (NeurIPS)*, pages 12544–12555, 2019.

[35] John M Lee. *Riemannian manifolds: an introduction to curvature*, volume 176. Springer Science & Business Media, 2006.

[36] James W Cannon, William J Floyd, Richard Kenyon, Walter R Parry, et al. Hyperbolic geometry. *Flavors of geometry*, 31(59-115):2, 1997.

[37] Yoshihiro Nagano, Shoichiro Yamaguchi, Yasuhiro Fujita, and Masanori Koyama. A wrapped normal distribution on hyperbolic space for gradient-based learning. In *International Conference on Machine Learning (ICML)*, pages 4693–4702, 2019.

[38] Emile Mathieu, Charline Le Lan, Chris J. Maddison, Ryota Tomioka, and Yee Whye Teh. Continuous hierarchical representations with poincaré variational auto-encoders. In *Neural Information Processing Systems (NeurIPS)*, pages 12544–12555, 2019.

[39] Jianxin Li, Xingcheng Fu, Qingyun Sun, Cheng Ji, Jiajun Tan, Jia Wu, and Hao Peng. Curvature graph generative adversarial networks. In *ACM Web Conference (WWW)*, pages 1528–1537, 2022.

[40] Abraham Albert Ungar. Analytic hyperbolic geometry: Mathematical foundations and applications. 2005.

[41] Tian Qi Chen, Yulia Rubanova, Jesse Bettencourt, and David Duvenaud. Neural ordinary differential equations. In *Neural Information Processing Systems (NeurIPS)*, pages 6572–6583, 2018.

[42] Baoquan Zhang, Xutao Li, Yunming Ye, Shanshan Feng, and Rui Ye. Metanode: Prototype optimization as a neural ode for few-shot learning. *arXiv preprint arXiv:2103.14341*, 2021.

[43] Chengming Xu, Yanwei Fu, Chen Liu, Chengjie Wang, Jilin Li, Feiyue Huang, Li Zhang, and Xiangyang Xue. Learning dynamic alignment via meta-filter for few-shot learning. In *IEEE/CVF Conference on Computer Vision and Pattern Recognition (CVPR)*, pages 5182–5191, 2021.

[44] Ernst Hairer, Syvert P. Nørsett, and Gerhard Wanner. Solving ordinary differential equations i: Nonstiff problems. *SIAM Rev.*, 32(3):485–486, 1990.

[45] Pierre-Antoine Absil, Robert E. Mahony, and Rodolphe Sepulchre. Optimization algorithms on matrix manifolds. 2007.

[46] Francisco Manuel Castro, Manuel J. Marín-Jiménez, Nicolás Guil Mata, Cordelia Schmid, and Alahari Karteek. End-to-end incremental learning. In *European Conference on Computer Vision (ECCV)*, pages 241–257, 2018.

[47] Saihui Hou, Xinyu Pan, Chen Change Loy, Zilei Wang, and Dahua Lin. Learning a unified classifier incrementally via rebalancing. In *IEEE/CVF Conference on Computer Vision and Pattern Recognition (CVPR)*, pages 831–839, 2019.

[48] Oriol Vinyals, Charles Blundell, Tim Lillicrap, Koray Kavukcuoglu, and Daan Wierstra. Matching networks for one shot learning. In *Neural Information Processing Systems (NeurIPS)*, pages 3630–3638, 2016.

[49] Mengye Ren, Eleni Triantafillou, Sachin Ravi, Jake Snell, Kevin Swersky, Joshua B. Tenenbaum, Hugo Larochelle, and Richard S. Zemel. Meta-learning for semi-supervised few-shot classification. In *International Conference on Learning Representations (ICLR)*, 2018.

[50] Alex Krizhevsky, Geoffrey Hinton, et al. Learning multiple layers of features from tiny images. 2009.

[51] Zitian Chen, Yanwei Fu, Yu-Xiong Wang, Lin Ma, Wei Liu, and Martial Hebert. Image deformation meta-networks for one-shot learning. In *IEEE/CVF Conference on Computer Vision and Pattern Recognition (CVPR)*, pages 8680–8689, 2019.

[52] Eli Schwartz, Leonid Karlinsky, Joseph Shtok, Sivan Harary, Mattias Marder, Abhishek Kumar, Rogério Schmidt Feris, Raja Giryes, and Alexander M. Bronstein. Delta-encoder: an effective sample synthesis method for few-shot object recognition. In *Neural Information Processing Systems (NeurIPS)*, pages 2850–2860, 2018.

[53] Hongguang Zhang, Jing Zhang, and Piotr Koniusz. Few-shot learning via saliency-guided hallucination of samples. In *IEEE/CVF Conference on Computer Vision and Pattern Recognition (CVPR)*, pages 2770–2779, 2019.

[54] Jian Zhang, Chenglong Zhao, Bingbing Ni, Minghao Xu, and Xiaokang Yang. Variational few-shot learning. In *IEEE/CVF International Conference on Computer Vision (ICCV)*, pages 1685–1694, 2019.

[55] Mengting Chen, Yuxin Fang, Xinggang Wang, Heng Luo, Yifeng Geng, Xinyu Zhang, Chang Huang, Wenyu Liu, and Bo Wang. Diversity transfer network for few-shot learning. In *AAAI Conference on Artificial Intelligence (AAAI)*, pages 10559–10566, 2020.

[56] Chelsea Finn, Pieter Abbeel, and Sergey Levine. Model-agnostic meta-learning for fast adaptation of deep networks. In *International Conference on Machine Learning (ICML)*, pages 1126–1135, 2017.

[57] Sungyong Baik, Seokil Hong, and Kyoung Mu Lee. Learning to forget for meta-learning. In *IEEE/CVF Conference on Computer Vision and Pattern Recognition (CVPR)*, pages 2379–2387, 2020.

[58] Sungyong Baik, Myungsub Choi, Janghoon Choi, Hee won Kim, and Kyoung Mu Lee. Meta-learning with adaptive hyperparameters. In *Neural Information Processing Systems (NeurIPS)*, pages 20755–20765, 2020.

[59] Sungyong Baik, Janghoon Choi, Heewon Kim, Dohee Cho, Jaesik Min, and Kyoung Mu Lee. Meta-learning with task-adaptive loss function for few-shot learning. In *IEEE/CVF International Conference on Computer Vision (ICCV)*, pages 9465–9474, 2021.

[60] Jake Snell, Kevin Swersky, and Richard Zemel. Prototypical networks for few-shot learning. In *Neural Information Processing Systems (NeurIPS)*, pages 4077–4087, 2017.

[61] Kwonjoon Lee, Subhransu Maji, Avinash Ravichandran, and Stefano Soatto. Meta-learning with differentiable convex optimization. In *IEEE/CVF Conference on Computer Vision and Pattern Recognition (CVPR)*, pages 10657–10665, 2019.

[62] Christian Simon, Piotr Koniusz, Richard Nock, and Mehrtash Harandi. Adaptive subspaces for few-shot learning. In *IEEE/CVF Conference on Computer Vision and Pattern Recognition (CVPR)*, pages 4136–4145, 2020.

[63] Sylvestre-Alvise Rebuffi, Alexander Kolesnikov, Georg Sperl, and Christoph H. Lampert. icarl: Incremental classifier and representation learning. In *IEEE/CVF Conference on Computer Vision and Pattern Recognition (CVPR)*, pages 5533–5542, 2017.

[64] Francisco M. Castro, Manuel J. Marín-Jiménez, Nicolás Guil, Cordelia Schmid, and Karteek Alahari. End-to-end incremental learning. In *European Conference on Computer Vision (ECCV)*, pages 241–257, 2018.

[65] Saihui Hou, Xinyu Pan, Chen Change Loy, Zilei Wang, and Dahua Lin. Learning a unified classifier incrementally via rebalancing. In *IEEE/CVF Conference on Computer Vision and Pattern Recognition (CVPR)*, pages 831–839, 2019.

[66] Rahaf Aljundi, Francesca Babiloni, Mohamed Elhoseiny, Marcus Rohrbach, and Tinne Tuytelaars. Memory aware synapses: Learning what (not) to forget. In *European Conference on Computer Vision (ECCV)*, pages 144–161, 2018.

[67] Prithviraj Dhar, Rajat Vikram Singh, Kuan-Chuan Peng, Ziyan Wu, and Rama Chellappa. Learning without memorizing. *IEEE/CVF Conference on Computer Vision and Pattern Recognition (CVPR)*, pages 5133–5141, 2019.

[68] Yu Liu, Sarah Parisot, Gregory G. Slabaugh, Xu Jia, Ale Leonardis, and Tinne Tuytelaars. More classifiers, less forgetting: A generic multi-classifier paradigm for incremental learning. In *European Conference on Computer Vision (ECCV)*, pages 699–716, 2020.

[69] Fei Zhu, Zhen Cheng, Xu-yao Zhang, and Cheng-lin Liu. Class-incremental learning via dual augmentation. In *Neural Information Processing Systems (NeurIPS)*, pages 14306–14318, 2021.

Checklist

1. For all authors...
   (a) Do the main claims made in the abstract and introduction accurately reflect the paper's contributions and scope? [Yes]
   (b) Did you describe the limitations of your work? [Yes] See Section 6.
   (c) Did you discuss any potential negative societal impacts of your work? [Yes]
   (d) Have you read the ethics review guidelines and ensured that your paper conforms to them? [Yes]
2. If you are including theoretical results...
   (a) Did you state the full set of assumptions of all theoretical results? [Yes]
   (b) Did you include complete proofs of all theoretical results? [Yes]
3. If you ran experiments...
   (a) Did you include the code, data, and instructions needed to reproduce the main experimental results (either in the supplemental material or as a URL)? [Yes]
   (b) Did you specify all the training details (e.g., data splits, hyperparameters, how they were chosen)? [Yes] See supplementary materials.
   (c) Did you report error bars (e.g., with respect to the random seed after running experiments multiple times)? [Yes] See experiments of few-shot learning.
   (d) Did you include the total amount of compute and the type of resources used (e.g., type of GPUs, internal cluster, or cloud provider)? [Yes] See supplementary materials.
4. If you are using existing assets (e.g., code, data, models) or curating/releasing new assets...
   (a) If your work uses existing assets, did you cite the creators? [Yes] See Section 5.1 and 5.2.
   (b) Did you mention the license of the assets? [No] The used datasets are publicly available, and widely used in existing few-shot learning and continual learning methods. Thus, we do not mention the license of the dataset.
   (c) Did you include any new assets either in the supplemental material or as a URL? [No]
   (d) Did you discuss whether and how consent was obtained from people whose data you're using/curating? [No] The used datasets are publicly available.
   (e) Did you discuss whether the data you are using/curating contains personally identifiable information or offensive content? [No] The used datasets does not contains personally identifiable information.

5. If you used crowdsourcing or conducted research with human subjects...
   (a) Did you include the full text of instructions given to participants and screenshots, if applicable? [N/A]
   (b) Did you describe any potential participant risks, with links to Institutional Review Board (IRB) approvals, if applicable? [N/A]
   (c) Did you include the estimated hourly wage paid to participants and the total amount spent on participant compensation? [N/A]